

# Adsorption of Cu(II) on maghnite from aqueous solution: Effects of pH, initial concentration, interaction time and temperature

Mohamed Amine Zenasni<sup>1,2\*</sup>, Said Benfarhi<sup>3</sup>, André Merlin<sup>2</sup>, Stéphane Molina<sup>2</sup>, Béatrice George<sup>2</sup>, Bahia Meroufel<sup>1,2</sup>

<sup>1</sup>Institute of Sciences and Technology, Department of Sciences, Bechar University, Bechar, Algeria;

\*Corresponding Author: [am.zenasni@gmail.com](mailto:am.zenasni@gmail.com)

<sup>2</sup>Laboratory of Studies and Research on Material Wood (LERMAB), University of Lorraine, Nancy, France

<sup>3</sup>Istitute of Sciences, Department of Chemistry, Batna University, Batna, Algeria

Received 19 September 2012; revised 20 October 2012; accepted 30 October 2012

## ABSTRACT

The adsorption behaviour of Cu<sup>2+</sup> onto maghnite was conducted under batch conditions. The effect of time, pH of the dispersion, temperature and initial metal concentration on the adsorption of Cu<sup>2+</sup> onto maghnite was investigated. In this study, 94% of Cu(II), was adsorbed on the maghnite clay when the equilibrium was reached at 120 min. The adsorption of Cu<sup>2+</sup> was a fast process that followed the pseudo-second-order kinetics. This process could be described by the Langmuir model and gave a maximum Cu<sup>2+</sup> adsorption capacity of 21.78 mg/g at 293 K. The thermodynamic parameters such as variation of enthalpy  $\Delta H$ , variation of entropy  $\Delta S$  and variation of Gibbs free energy  $\Delta G$  were calculated from the slope and intercept of  $\ln K_d$  vs.  $1/T$  plots. The adsorption was endothermic reaction. The adsorption process for this natural maghnite is more spontaneous because the values of  $\Delta G$  are less negative. The results suggested that natural maghnite was suitable as sorbent material for the recovery and adsorption of metal ion from aqueous solutions.

**Keywords:** Adsorption; Isotherms; Natural Maghnite; Heavy Metal; Cu(II)

## 1. INTRODUCTION

Many toxic heavy metals have been discharged to the environment as industrial wastes, causing serious soil and water pollution [1]. Over the past few decades the huge increase in the use of heavy metals has resulted in an increased flux of metallic substances in aquatic environment.

They are also common groundwater contaminants at industrial and military installations. Heavy metal ions can be removed by several ways, e.g., precipitation and sorption by various media. The choice of which media depends upon the type and concentration of both sorptive material and sorbent employed, as well as their costs.

In the recent years the adsorption of heavy metals by a variety of substances has been the subject of many studies. One of the powerful treatment processes for the removal of metal ions from water with a low cost is adsorption. Several adsorbents are eligible for such a purpose. Activated carbon is the most popular adsorbent and has been used with great success [2]. A large number of low-cost adsorbents have been treated for metal ions removal. Other known natural materials like clay and zeolite have been investigated for their potential use of adsorbents for heavy metal [3,4].

Clays (especially maghnite) are widely used to study the adsorption of pollutants. These clays are chosen to avoid pollutant release into the environment, low cost and ubiquitous presence in most soils. Maghnite as a representative clay mineral is a clay mainly composed of montmorillonite, a 2:1 type of aluminosilicate. Maghnite is highly valued for their sorption [5].

The reactions of metals at the solid-solution interface play important role in determining their treatment by adsorption process, as well as in determining their fate in the environment [6,7]. These reactions which include adsorption, precipitation and polymerisation are often collectively called sorption [7]. Adsorption is a much faster process than precipitation. Adsorption of metals at mineral-water interface is often initially fast followed by a decrease in the adsorption rate [6,8].

The objective of the research described here was to investigate sorption characteristics of Cu<sup>2+</sup> onto maghnite. The ability of maghnite to adsorb metal ions in solution

was shown as a function of some experimental parameters. Values of well-known thermodynamic functions and isotherm studies for adsorption of  $\text{Cu}^{2+}$  onto maghnite have been investigated and reported.

## 2. MATERIALS AND METHODS

### 2.1. Clay Minerals

The maghnite used in this work came from a quarry located in Maghnia (North West of Algeria) and was supplied by company "ENOF" (an Algerian manufacture specialized in the production of nonferrous products and useful substances). The different chemical elements of the native maghnite were transformed into oxides and analysed by X-ray fluorescence (experiment carried out at ENOF). Results are given in **Table 1**. These results confirm that the maghnite used consists essentially of montmorillonite, since the ratio  $\text{SiO}_2/\text{Al}_2\text{O}_3$  is equal to 3.77 and thus belongs to the family of the phyllosilicates. This maghnite form is stable suspensions in water and had flat platelets or needle-like structures. Granulometry of the crude maghnite have been prepared in the Civil Engineering Department of Tlemcen University (EDTU) in Algeria using a sedimentation technique with a 0.1% solution of sodium hexametaphosphate; 95% of the particles were found to have a diameter of less than 80  $\mu\text{m}$ . The cation exchange capacity was measured to be 101.25 meq/100g of clay, and the surface area was 27  $\text{m}^2/\text{g}$ , with an average pore size of 7 nm [9,10].

### 2.2. Reagents

The reagents used in this study were all extra pure analytical grades:  $\text{CuSO}_4 \cdot 5\text{H}_2\text{O}$ , NaOH (0.1 M) and HCl (0.1 M). A stock of Cu(II) solution of 1000 ppm, were prepared by dissolving 3.929 g of  $\text{CuSO}_4 \cdot 5\text{H}_2\text{O}$  (Fluka) in 1 L of deionized water. The range of concentrations prepared from stock solution was varied. The pH of solution was adjusted by using 0.1 M NaOH and/or 0.1 M HCl.

### 2.3. Instrumentation

The pH of all solution was measured by a TitraLab Instrument TIM800 Model pH meter. The adsorption experiments have been studied by batch technique using a thermostated shaker bath GFL-1083 Model. A Eppendorf 5702 Model digital centrifuge was used to centrifuge the samples. Cu(II) concentrations of solutions before and

after adsorption were measured by using flame atomic absorption spectrophotometer (Varian, SpectrAA-100, AAS).

The Fourier transform infrared (FT-IR) spectra using KBr pressed disk technique were conducted by Perkin Elmer Spectrum 2000 Infrared spectrometer. Natural maghnite and KBr were weighted and then were ground in an agate mortar for 10 min prior to pellet making. The spectrums were collected for each measurement over the spectral range of 400 - 4000  $\text{cm}^{-1}$ .

TG-DTA thermograms were plotted using the multi-module 92 - 10 Setaram analyser operating from room temperature up to 1000°C in a  $\text{Al}_2\text{O}_3$  crucible, at 10°C/mn heating rate.

Nanomorphology was characterized by scanning electron microscopy (SEM) and transmission electron microscopy (TEM). The SEM study was carried out using Hitachi S-4800 equipped with energy dispersive spectrometry for chemical analysis (EDS) and operating at 15 kV acceleration voltage. TEM study was performed with a Philips CM10 microscope operating at 100 kV.

### 2.4. Adsorption Study

The effect of contact time on the adsorption capacity of maghnite was studied in the range 1 - 360 min at an initial concentration of 100 mg/L. Adsorption kinetics was studied using an initial concentration of 100 mg/L with the sorbent dosage of 0.2 g/20 mL at pH 5.5. Adsorption isotherms were studied at various initial concentrations of Cu(II) ion in the range of 10 - 500 mg/L and the experiments were conducted at different constant temperatures in the range 20°C - 60°C. The maximum adsorption capacity was calculated from Langmuir, Freundlich and Dubinin-Radushkevich isotherms plot. The amount of Cu(II) adsorbed per unit mass of maghnite was calculated by using the mass balance equation given in **Eq. 1** [11].

$$q_e = \frac{(C_0 - C_e)V}{m} \quad (1)$$

where  $q_e$  is the maximum adsorption capacity in mg/g,  $C_0$  is the initial concentration and  $C_e$  is the concentration at equilibrium of Cu(II) solution in mg/L,  $V$  is the volume of the Cu(II) solution in mL and  $m$  is the mass of the maghnite in grams.

Adsorption percentage (%) was derived from the difference of the initial concentration ( $C_0$ , mol/L) and the final one ( $C_e$ , mol/L) (**Eq. 2**):

**Table 1.** Chemical composition of the maghnite.

Species	$\text{SiO}_2$	$\text{Al}_2\text{O}_3$	$\text{Fe}_2\text{O}_3$	CaO	MgO	$\text{Na}_2\text{O}$	$\text{K}_2\text{O}$	$\text{TiO}_2$	L.O.I*
% (w/w)	65.20	17.25	2.10	1.20	3.10	2.15	0.60	0.20	8.20

\*Loss on ignition.

$$\text{Sorption\%} = \frac{C_0 - C_e}{C_0} \times 100\% \quad (2)$$

### 3. RESULTS AND DISCUSSION

#### 3.1. Properties of Natural Maghnite

Chemical analysis data of the natural maghnite are presented in **Table 1**.

This study showed that natural maghnite contained sodium, potassium and calcium ions. Low-silica members are enriched with calcium, where as high-silica montmorillonite are enriched with potassium, sodium and magnesium.

FT-IR studies of these adsorbents help the identification of various forms of the minerals that are present in the clay. Infrared spectra of the charge maghnite, illustrated in **Figure 1**, show the presence of absorption bands of clay phase and absorption characteristic bands of impurities.

A strong band at  $3623.90 \text{ cm}^{-1}$  and  $3464.43 \text{ cm}^{-1}$  indicates the possibility of the hydroxyl linkage. However, a broad band at  $3464.43 \text{ cm}^{-1}$  and a band at  $1631.34 \text{ cm}^{-1}$  in the spectrum of clay suggest the possibility of water of hydration in the adsorbent. The bands due to free (or weakly hydrogen-bonded water molecule to the surface oxygen of tetrahedral sheet) water molecules, water-water hydrogen bond ( $\text{M}^{\text{n}+}\text{-O-H-O-H-}$ ) and water bending modes are observed near  $3623.90$ ,  $3464.43$  and  $1631.34 \text{ cm}^{-1}$ , respectively. The strong band near  $1037.10 \text{ cm}^{-1}$  is due to Si-O-Si stretching vibration in tetrahedral sheets,

which corresponds to the characteristic band of montmorillonite [12]. The coupled vibrations are appreciable due to the availability of various constituents. In the IR studies of maghnite, the Si-O stretching vibrations were observed at  $697.86 \text{ cm}^{-1}$ ,  $524.86 \text{ cm}^{-1}$  and  $469.95 \text{ cm}^{-1}$  showing the presence of quartz. The appearance of  $\nu$  (Si-O-Si) and  $\delta$  (Si-O) bands also support the presence of quartz [13]. The vibrations observed at  $912.24 \text{ cm}^{-1}$  indicate the possibility of the presence of hematite [14].

Result from thermal analysis is reported in **Figure 2**. The TG curve of the natural maghnite shows three main steps of weight loss. In the first step ( $T < 200^\circ\text{C}$ ) a weight loss (about 18.50%) corresponding to both adsorbed and interlayer water loss takes place. After this step, the TG curve shows a slight gradual decrease (about 2.10%) in the range  $200^\circ\text{C} - 580^\circ\text{C}$ , which is attributed to the water loss of maghnite. Finally, a third main loss occurs at temperatures in the range  $580^\circ\text{C} - 900^\circ\text{C}$ , where the TG curve displays a step weight loss (about 4.11%) related to the release of structural OH of natural maghnite. The dehydroxylation temperature of about  $650^\circ\text{C}$  (see **Figure 2**) is in agreement with the classical range of dehydroxylation temperature ( $600^\circ\text{C} - 700^\circ\text{C}$ ) observed by various authors for cis vacant montmorillonites [15].

SEM micrograph of the untreated maghnite sample suggests a very cohesive material (**Figure 3**). The micrograph confirms that the material is forming micron-size agglomerates. A higher magnification micrograph of the same structure shows that the micro-size particles are composed of individual platelets, which conglomerate into larger size particles.

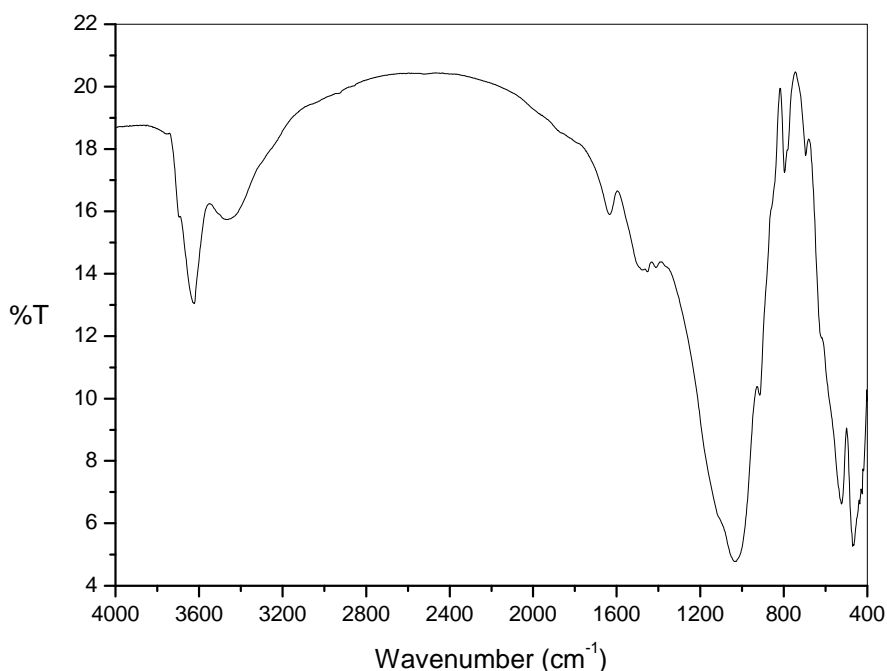


**Figure 1.** Infrared (IR) spectra of natural maghnite.

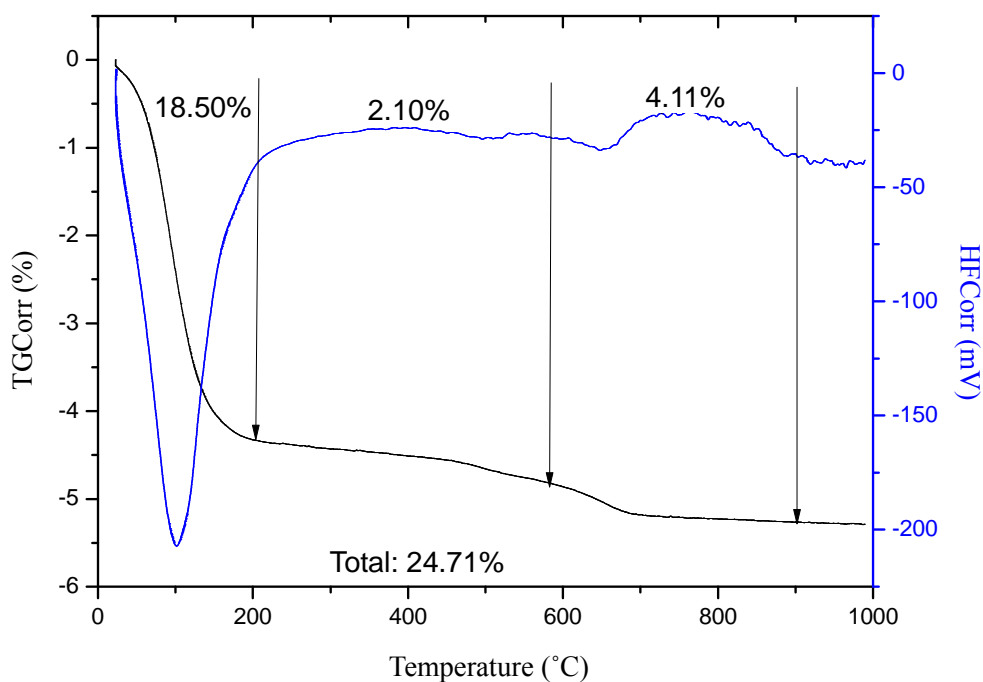


Figure 2. TG-DTA analyse of natural maghnite.

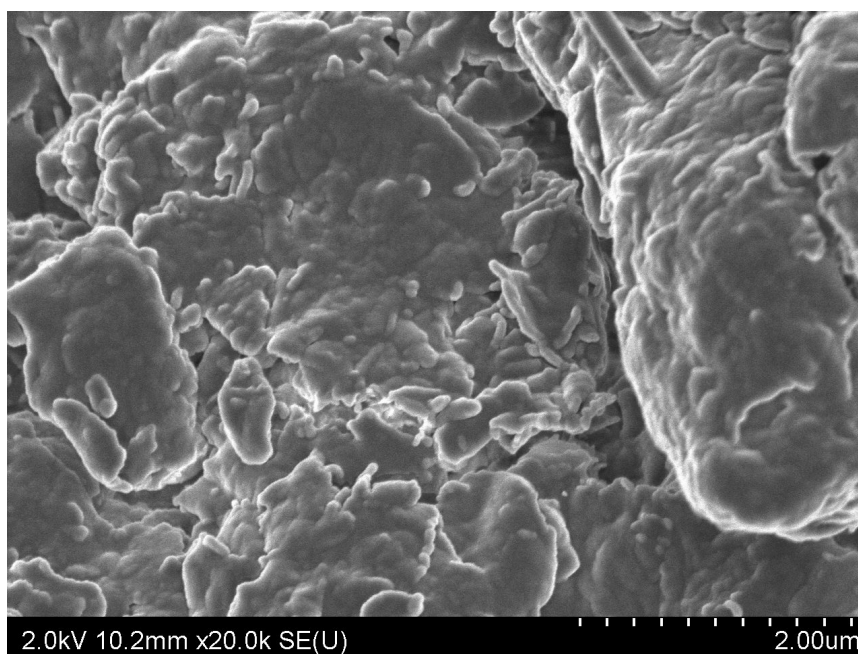


Figure 3. SEM image of maghnite sample.

The obtained chemical analysis by energy dispersive spectroscopy (Figure 4) shows the presence of framework Al and Si elements. The molar Si/Al ratio for used maghnite is about 2.78. The presence also of the Na, K and Mg elements in the structure of maghnite.

The TEM micrographs at low magnification showed (Figure 5) a higher tendency of the maghnite to aggregate.

### 3.2. Effect of Initial Concentration of Cu(II)

Effect of initial concentration of Cu(II) on adsorption capacity of maghnite was investigated by varying initial concentration of Cu(II) from 10 to 500 mg/L. For this study, pH, temperature, adsorbent dosage and contact time have been fixed as 20°C, 0.2 g/20mL and 24 h. The results are presented in Figure 6. An increase of Cu(II)

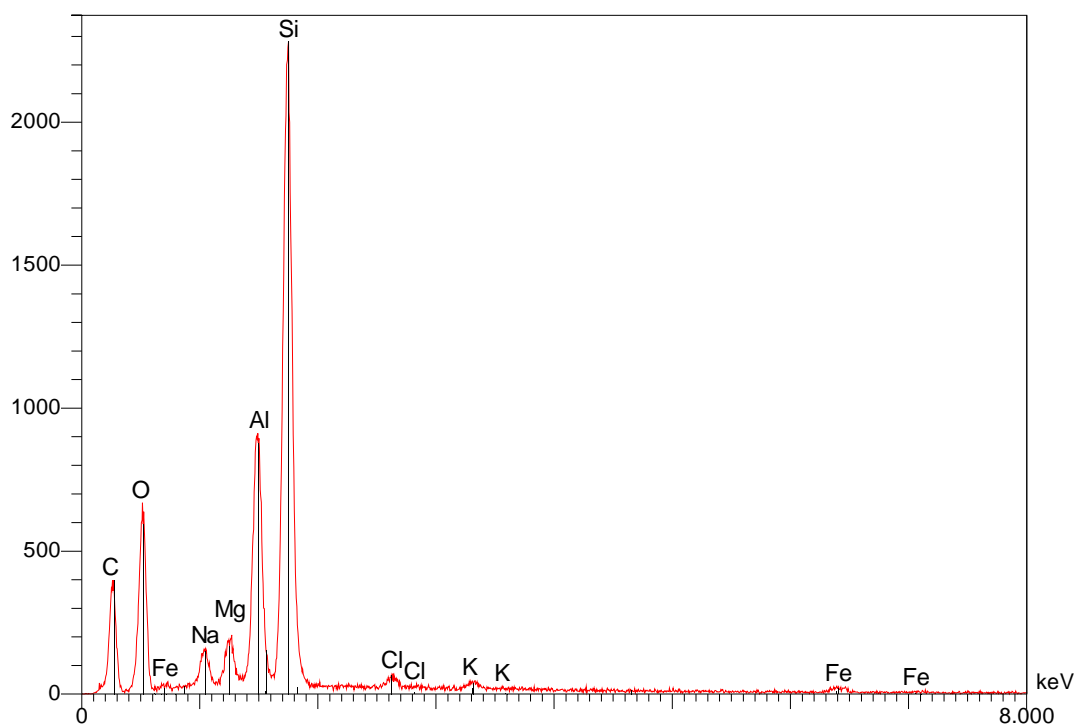


**Figure 4.** SEM-EDS spectra of maghnite sample.

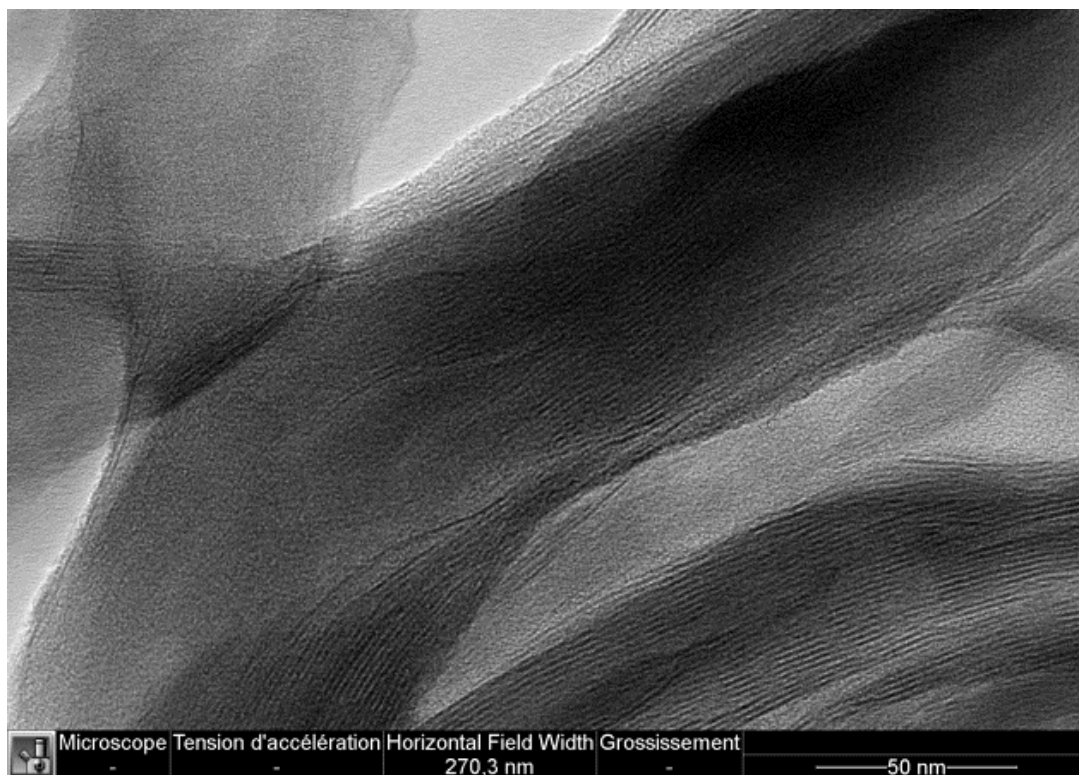


**Figure 5.** TEM micrograph of the maghnite.

concentration accelerates the diffusion of Cu(II) ions from solution to the adsorbent surface due to the increase in driving force of concentration gradient. Hence, the

amount of adsorbed Cu(II) at equilibrium increased from 0.99 to 21.6 mg/g as the Cu(II) concentration is increased from 10 to 500 mg/L.

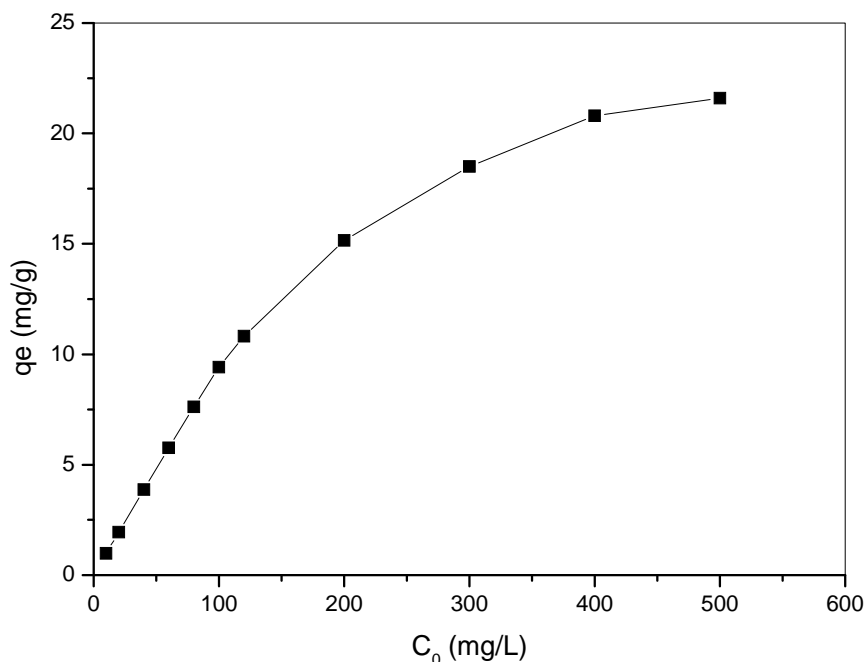


Figure 6. Effect of initial concentration of Cu(II) on adsorption capacity of maghnite.

### 3.3. Effect of Initial pH on Adsorption Capacity of Maghnite

Effect of initial pH on the adsorption capacity of maghnite for Cu(II) was studied by varying solution pH from 1.5 to 5.5 at the adsorbent dosage of 0.2 g/20mL using an initial concentration of Cu(II) as 100 mg/L. The pH range of 1.5 - 5.5 was chosen, as the precipitation of Cu(II) is found to occur at  $\text{pH} \geq 6$  [16]. Variation of adsorption capacity of maghnite for Cu(II) ions with pH is shown in Figure 7. It is evident that the adsorption of Cu(II) ions on maghnite is strongly dependant on the pH of the solution. The adsorption of Cu(II) ions increases steadily with increase in initial pH from 1.5 to 5.5 and the maximum adsorption capacity of 9.94 mg/g is observed at pH 5.5.

### 3.4. Effects of Interaction Time and Kinetics of Adsorption

The adsorption of Cu(II) on maghnite as a function of contact time at  $\text{pH } 5.5 \pm 0.1$  is shown in Figure 8.

The Cu(II) interacted with the maghnite rapidly and within 40 min, the maximum uptake was observed (Figure 8). Afterwards, the interactions slowed down and approached equilibrium in nearly 120 min under the given set of experimental conditions.

Attainment of equilibrium is influenced by several factors including the nature of the adsorbent and the adsorbate, and the interactions between them.

Initially, the rate of adsorption on the bare surface was very high, but as the sites got covered with the Cu(II),

the rate decreased. The rate now becomes predominantly dependent on the rate at which metal ions are transported from the bulk liquid phase to the adsorbent-adsorbate interface. The kinetics of the interactions is thus likely to be dependent on different rate processes as the interaction time increases [17].

In this study, 94% of Cu(II), was adsorbed on the maghnite clay when the equilibrium was reached at 120 min. On the basis of this result, it can be observed that natural maghnite clay can be used to remove this metal ion.

The fast adsorption of Cu(II) on maghnite suggested that the uptake of Cu(II) from solution to maghnite was mainly dominated by chemical adsorption rather than physical adsorption [18,19].

To analyze the kinetic adsorption of Cu(II) on maghnite, a pseudo-second-order rate equation was used to simulate the kinetic adsorption (Eq. 3) [20]:

$$\frac{t}{q_t} = \frac{1}{2K'q_e^2} + \frac{1}{q_e}t \quad (3)$$

where  $q_t$  (mg/g) is the amount of Cu(II) adsorbed on maghnite at time  $t$  (min),  $q_e$  (mg/g) is the equilibrium adsorption capacity and  $K'$  (g/(mg·min)) is the pseudo-second-order rate constant of adsorption. The values of  $K'$  and  $q_e$  calculated from the intercept and slope of equation are 0.19 g/(mg·min) and 9.43 mg/g, respectively. The correlation coefficient of the pseudo-second-order rate equation for the linear plot is 1.00 (see Figure 9), which suggests that the kinetic adsorption can be described by the pseudo-second-order rate equation.

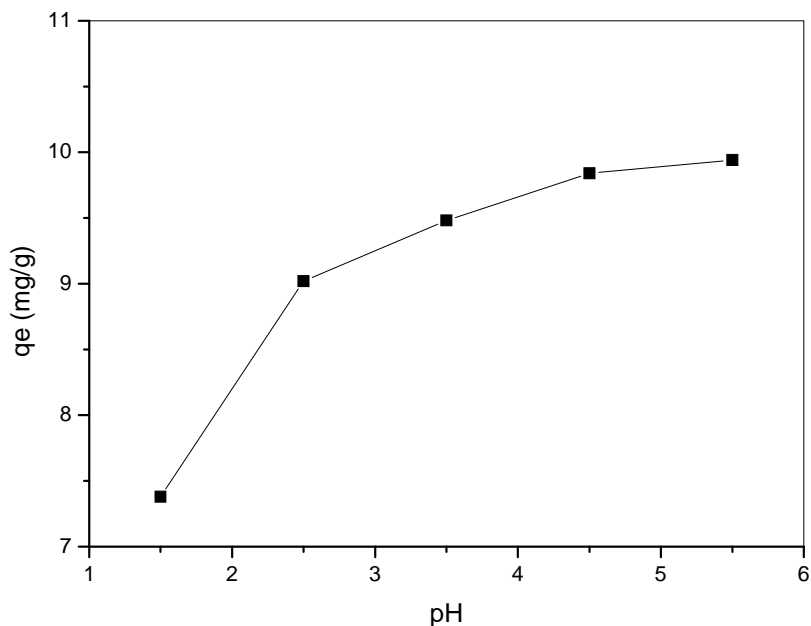


Figure 7. Effect of pH on adsorption capacity of maghnite for Cu(II).

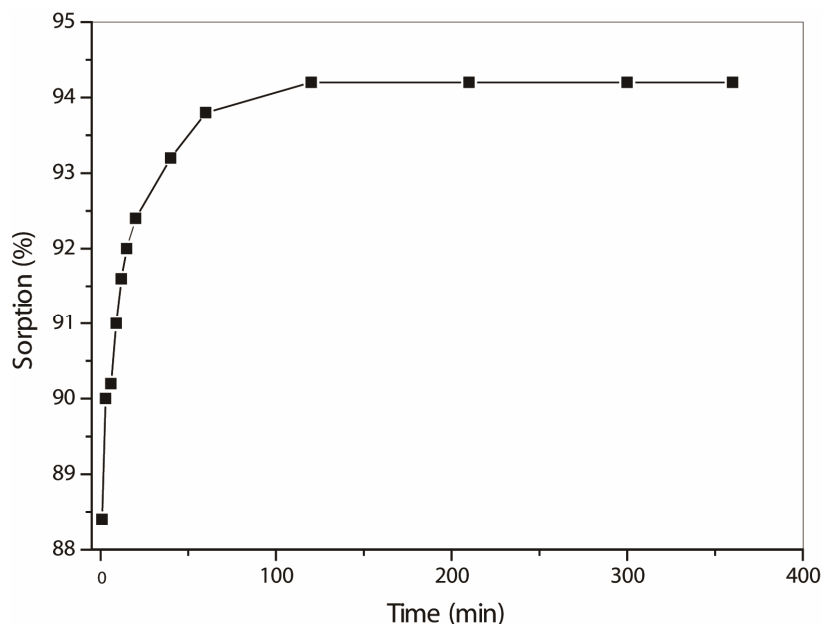


Figure 8. Effect of contact time on the adsorption of Cu(II) to natural maghnite, pH = 5.5 ± 0.1, T = 293 K, clay 10 g/L, C[Cu(II)]initial = 100 mg/L.

### 3.5. Construction of Isotherms and Model Fitting

Sorption isotherms were constructed by plotting the amount of metal sorbed (mg/g) against the equilibrium concentration of metal in solution (mg/L).

Three models have been adopted in this paper, namely: Langmuir, Freundlich and Dubinin- Radushkevich (D-R) equilibrium isotherm models. The Langmuir and Freundlich isotherms are used most commonly to describe the

adsorption characteristics of metal ions in water and wastewater treatment [21].

#### 3.5.1. Langmuir Isotherm

The data conform the linear form of Langmuir model (Eq. 4) [22] expressed below:

$$\frac{C_e}{q_e} = \frac{C_e}{q_m} + \frac{1}{K_L q_m} \quad (4)$$

where  $C_e$  is equilibrium concentration of Cu(II) (mg/L)

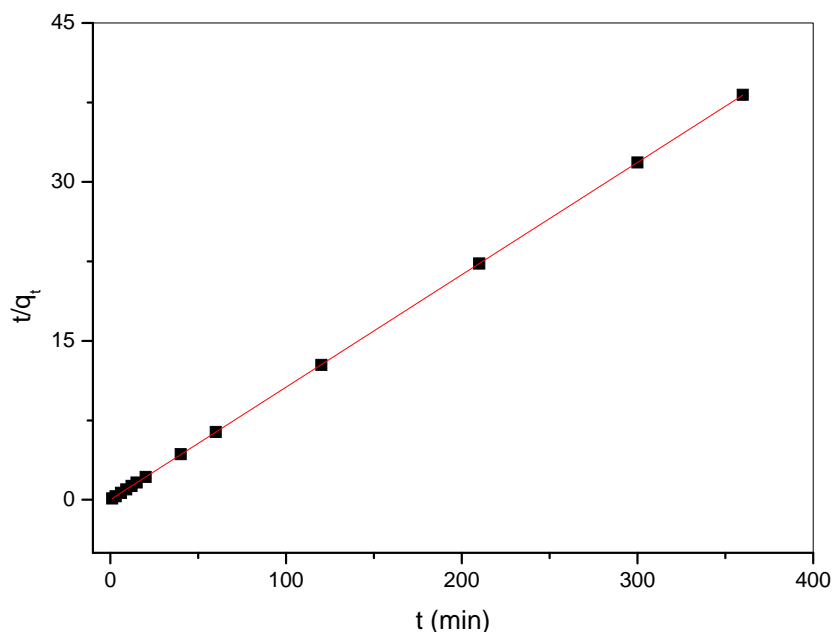


**Figure 9.** Lagergren pseudo second-order plots for Cu(II) adsorbed on maghnite at 293K, pH (5.5).

and  $q_e$  is the amount of the  $\text{Cu}^{2+}$  adsorbed (mg) by per unit of maghnite (g).  $q_m$  and  $K_L$  are the Langmuir constants related to the adsorption capacity (mg/g) and the equilibrium constant (L/g), respectively. The Langmuir monolayer adsorption capacity ( $q_m$ ) gives the amount of the metal required to occupy all the available sites per unit mass of the sample (see **Figure 10**). The Langmuir monolayer adsorption capacities of maghnite was estimated as 21.78 mg/g, (**Table 2**). The value of maximum adsorption capacity ( $q_m$ ) calculated from the Langmuir isotherm in this study is much higher than that of those reported in the literature. For example, adsorption of Cu(II) at 308 K on waste iron oxide follows the Langmuir isotherm model with an adsorption capacity of 14.10 mg/g [23]. Langmuir adsorption capacity for Cu(II) adsorption on shells of lentil, wheat, and rice has been shown to be 8.97, 16.07 and 2.31 mg/g, respectively, by Aydın et al. [24]. The uptake of Cu(II) on spent activated clay has Langmuir monolayer capacity  $q_m = 13.2$  mg/g at pH 6.0 [25].

### 3.5.2. Freundlich Isotherm

The adsorption equilibrium data was also applied to the Freundlich model (**Eq. 5**) [26] given below:

$$\log q_e = \log K_f + \left(\frac{1}{n}\right) \log C_e \quad (5)$$

where  $K_f$  and  $n$  are Freundlich constants related to adsorption capacity and adsorption intensity, respectively. Freundlich parameters ( $K_f$  and  $n$ ) indicate whether the nature of adsorption is either favorable or unfavorable.

The intercept is an indicator of adsorption capacity and the slope is an indicator of adsorption intensity. A relatively slight slope  $n \ll 1$  indicates that adsorption intensity is good (or favorable) over the entire range of concentrations studied, while a steep slope ( $n > 1$ ) means that adsorption intensity is good (or favorable) at high concentrations but much less at lower concentrations [27]. A high value of the intercept,  $K_f$ , is indicative of a high adsorption capacity. In the adsorption system,  $n$  value is 2.63 which indicates that adsorption intensity is good (or favorable) over the entire range of concentrations studied. The  $K_f$  value of the Freundlich equation (**Table 2**) also indicates that maghnite has a very high adsorption capacity for copper ions in aqueous solutions (see **Figure 11**).

### 3.5.3. Dubinin-Radushkevich (D-R)

The equilibrium data were also applied to the Dubinin-Radushkevich (D-R) isotherm model to determine if adsorption occurred by physical or chemical processes. The linearized form of the D-R isotherm [28-32] is as follows (**Eq. 6**):

$$\ln q_e = \ln q_m - \beta \varepsilon^2 \quad (6)$$

where  $\beta$  is the activity coefficient related to mean adsorption energy ( $\text{mol}^2/\text{J}^2$ ) and  $\varepsilon$  is the Polanyi potential (**Eq. 7**):

$$\varepsilon = RT \ln \left( 1 + \frac{1}{C_e} \right) \quad (7)$$

The D-R isotherm is applied to the data obtained from



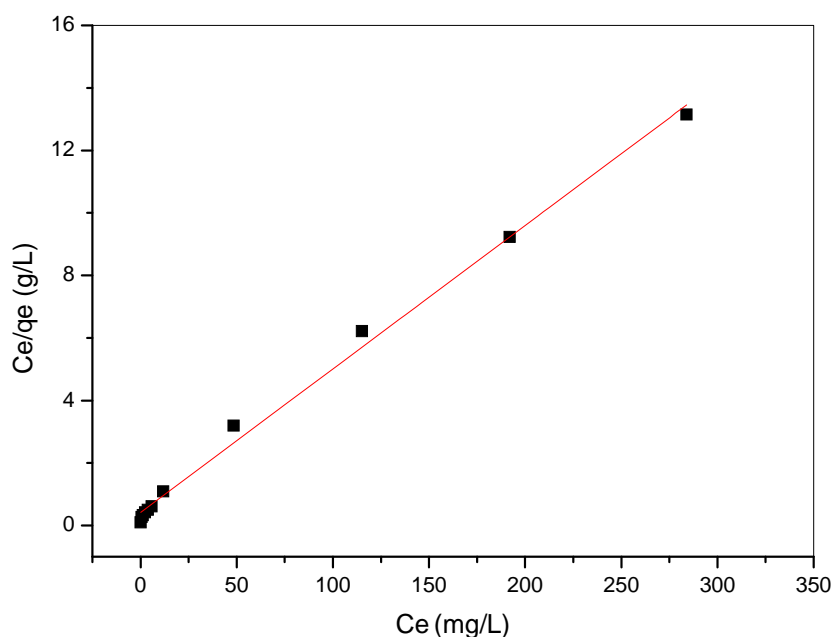


**Figure 10.** Langmuir isotherm plot for adsorption of  $\text{Cu}^{2+}$  on the maghnite.  $T = 293$  K, initial pH 5.5,  $m/V = 10$  g/L.

**Table 2.** Langmuir, Freundlich and D-R isotherm parameters for the adsorption of  $\text{Cu}^{2+}$  onto maghnite sample.

Sample	Langmuir isotherm constants			Freundlich isotherm constants			D-R isotherm constants		
	$q_m$ (mg/g)	$K_L$ (L/g)	$R^2$	$n$	$K_f$	$R^2$	$q_m$ (mg/g)	$E$ (kJ/mol)	$R^2$
Maghnite	21.78	0.11	0.995	2.63	3.36	0.967	10.2	2.55	0.564

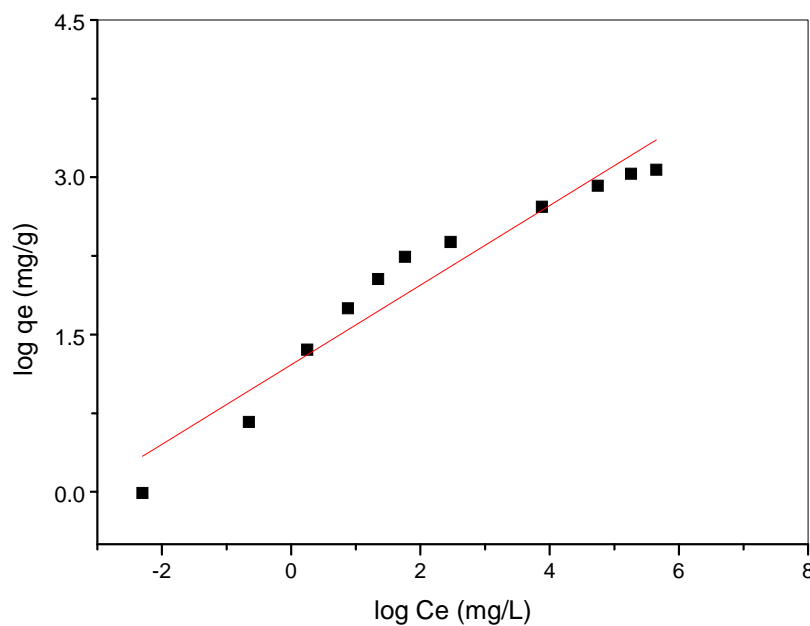


**Figure 11.** Freundlich isotherm plot for adsorption of  $\text{Cu}^{2+}$  on the maghnite.  $T = 293$  K, initial pH 5.5,  $m/V = 10$  g/L.

the empirical studies. A plot of  $\ln q_e$  against  $\varepsilon^2$  is given in **Figure 12**. D-R isotherm constants,  $q_m$ , for maghnite was

found to be 10.2 mg/g (**Table 2**).

The difference of  $q_m$  derived from the Langmuir and

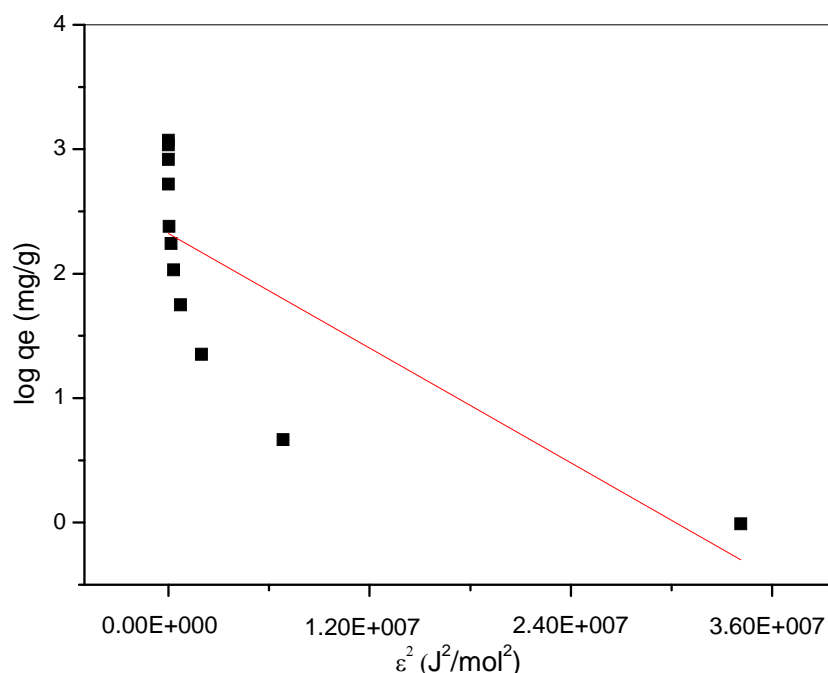


**Figure 12.** D-R isotherm plot for adsorption of  $\text{Cu}^{2+}$  on the maghnite.  $T = 293$  K, initial pH 5.5,  $m = 10$  g/L.

D-R models is large. The difference may be attributed to the different definition of  $q_m$  in the two models. In Langmuir model,  $q_m$  represents the maximum adsorption of metal ions at monolayer coverage, whereas it represents the maximum adsorption of metal ions at the total specific micropore volume of the adsorbent in D-R model. Thereby, the value of  $q_m$  derived from Langmuir model is higher than that derived from D-R model. The differences are also reported in previous studies [28,30]. The mean adsorption energy,  $E$  (kJ/mol) is as follows (Eq. 8):

$$E = \frac{1}{\sqrt{-2\beta}} \quad (8)$$

This adsorption potential is independent of the temperature, but it varies depending on the nature of adsorbent and adsorbate. The magnitude of  $E$  is used for estimating the type of adsorption mechanism. If the  $E$  value is between 8 and 16 kJ/mol, the adsorption process follows by chemical adsorption and if  $E < 8$  kJ/mol, the adsorption process is of a physical nature [28-32]. The calculated values of  $E$  are 2.55 kJ/mol for maghnite, and they are in the range of values for physical adsorption reactions. The similar results for the adsorption of Cu(II) was reported by earlier worker [27].

### 3.6. Thermodynamic Studies

Using the following equations, the thermodynamic parameters of the adsorption process were determined

from the experimental data (Eqs. 9-11):

$$\ln K_d = \frac{\Delta S}{R} - \frac{\Delta H}{RT} \quad (9)$$

$$\Delta G = \Delta H - T\Delta S \quad (10)$$

$$K_d = \frac{q_e}{C_e} \quad (11)$$

where  $K_d$  is the distribution coefficient for the adsorption,  $\Delta S$ ,  $\Delta H$  and  $\Delta G$  are the changes of entropy, enthalpy and the Gibbs energy,  $T$  (K) is the temperature,  $R$  ( $\text{J}\cdot\text{mol}^{-1}\cdot\text{K}^{-1}$ ) is the gas constant. The values of  $\Delta H$  and  $\Delta S$  were determined from the slopes and intercepts of the plots of  $\ln K_d$  vs.  $1/T$  (show Figure 13).

The negative values for the Gibbs free energy change,  $\Delta G$ , show that the adsorption process for the maghnite is spontaneous and the degree of spontaneity of the reaction increases with increasing temperature. The increase in adsorption with temperature may be attributed to either increase in the number of active surface sites available for adsorption on the adsorbent or the desolvation of the adsorbing species and the decrease in the thickness of the boundary layer surrounding the adsorbent with temperature, so that the mass transfer resistance of adsorbate in the boundary layer decreases. The values of  $\Delta G$  are less negative for the maghnite suggesting that the adsorption process for this material is more spontaneous. These results suggest that the internal domains of this sample are more suitable environments for Cu(II) cations than the maghnite. The data shown in Table 3 show that the heats

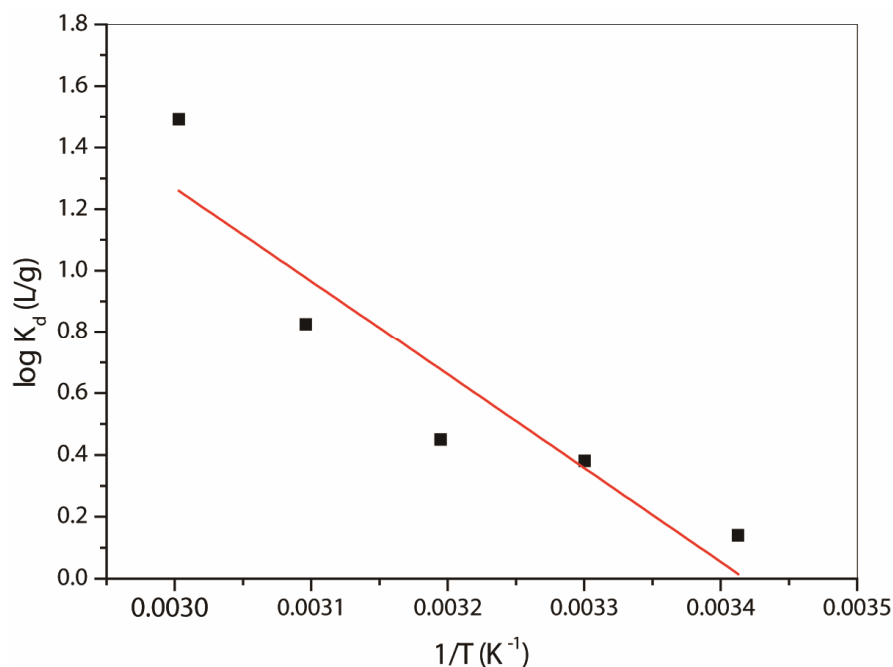


**Figure 13.** Plot of  $\ln K_d$  against  $1/T$  for the adsorption of Cu(II) on maghnite.

**Table 3.** Thermodynamic parameters for the adsorption of Cu(II) onto maghnite.

Sample	$\Delta H$ (kJ/mol)	$\Delta S$ (J/mol K)	$\Delta G$ (kJ/mol)					$R^2$
			293 K	303 K	313 K	323 K	333 K	
Maghnite	25.22	86.22	-0.042	-0.905	-1.767	-2.629	-3.491	0.826

of adsorption are positive for both types of the maghnite. These positive value of  $\Delta H$  indicate the endothermic behavior of the adsorption reaction of Cu(II) ions and suggest that a large amount of heat is consumed to transfer the Cu(II) ions from aqueous into the solid phase. As was suggested by Nunes and Airoidi [33], the transition metal ions must give up a larger share of their hydration water before they could enter the smaller cavities. Such a release of water from the divalent cations would result in positive value of  $\Delta S$ . This mechanism of the adsorption of Cu(II) ions is also supported by the positive value of  $\Delta S$ , which show that Cu(II) ions are less hydrated in the maghnite layers than in the aqueous solution. Also, the positive value of  $\Delta S$  indicates the increased disorder in the system with changes in the hydration of the adsorbing Cu(II) cations.

#### 4. CONCLUSION

The adsorption of Cu(II) depends upon the nature of the adsorbent surface and the species distribution of Cu(II) in solution, which mainly depends on the pH of the system. The plots have good linearity in both the cases (Freundlich plot,  $R^2 = 0.967$ , Langmuir plot,  $R^2 = 0.995$ ) at 298 K. The values of the adsorption coefficients

indicate the favorable nature of adsorption of Cu(II) on the natural maghnite.

#### 5. ACKNOWLEDGEMENTS

The authors gratefully acknowledge to the Dr Yves PILLET (Faculty of Sciences et Technology, group PGCM, University of Lorraine, Nancy, France) because of contribution to our study, and thankful for Joint Service Electronic Microscopy and Microanalysis at the University Henri Poincare of Nancy for MEB-EDS analysis.

#### REFERENCES

- [1] Jiang, M.Q., Jin, X.Y., Lu, X.Q. and Chen, Z.L. (2010) Adsorption of Pb(II), Cd(II), Ni(II) and Cu(II) onto natural kaolinite clay. *Desalination*, **252**, 33-39. [doi:10.1016/j.desal.2009.11.005](https://doi.org/10.1016/j.desal.2009.11.005)
- [2] LI, Y., Huang, Z.H., Kang, F.Y. and Li, B.H. (2010) Preparation of activated carbon microspheres from phenolic resin with metal compounds by sub- and supercritical water activation. *New Carbon Materials*, **25**, 109-113. [doi:10.1016/S1872-5805\(09\)60019-6](https://doi.org/10.1016/S1872-5805(09)60019-6)
- [3] Salem, A. and Akbari Sene R. (2011) Removal of lead from solution by combination of natural zeolite-kaolinite-bentonite as a new low-cost adsorbent. *Chemical Engineering Journal*, **174**, 619-628. [doi:10.1016/j.cej.2011.09.075](https://doi.org/10.1016/j.cej.2011.09.075)

- [4] Yousef, R.I., El-Eswed, B. and Al-Muhtaseb, A.H. (2011) Adsorption characteristics of natural zeolites as solid adsorbents for phenol removal from aqueous solutions: Kinetics, mechanism, and thermodynamics studies. *Chemical Engineering Journal*, **171**, 1143-1149. [doi:10.1016/j.cej.2011.05.012](https://doi.org/10.1016/j.cej.2011.05.012)
- [5] Harrane, A., Belaouedj, M.A. and Belbachir, M. (2011) Cationic ring-opening polymerization of (d,l-lactide) using Maghnite-H<sup>+</sup>, a non-toxic catalyst. *Reactive and Functional Polymers*, **71**, 126-130. [doi:10.1016/j.reactfunctpolym.2010.11.022](https://doi.org/10.1016/j.reactfunctpolym.2010.11.022)
- [6] Bhattacharyya, K.G. and Gupta, S.S. (2008) Adsorption of a few heavy metals on natural and modified kaolinite and montmorillonite: A review. *Advances in Colloid and Interface Science*, **140**, 114-131. [doi:10.1016/j.cis.2007.12.008](https://doi.org/10.1016/j.cis.2007.12.008)
- [7] Anirudhan, T.S. and Suchithra, P.S. (2010) Heavy metals uptake from aqueous solutions and industrial wastewaters by humic acid-immobilized polymer/bentonite composite: Kinetics and equilibrium modeling. *Chemical Engineering Journal*, **156**, 146-156. [doi:10.1016/j.cej.2009.10.011](https://doi.org/10.1016/j.cej.2009.10.011)
- [8] Sdiri, A., Higashi, T., Hatta, T., Jamoussi, F. and Tase, N. (2011) Evaluating the adsorptive capacity of montmorillonitic and calcareous clays on the removal of several heavy metals in aqueous systems. *Chemical Engineering Journal*, **172**, 37-46. [doi:10.1016/j.cej.2011.05.015](https://doi.org/10.1016/j.cej.2011.05.015)
- [9] Zenasni, M.A., Benfarhi, S. and Meroufel, B. (2011) Effect of the degree of ionization on the insertion of polyvinylpyridinium salts into Bentonite. *Hindawi Publishing Corporation, International Journal of Inorganic Chemistry*, Article ID 723020, 1-6. [doi:10.1155/2011/723020](https://doi.org/10.1155/2011/723020)
- [10] Zenasni, M.A., Benfarhi, S., Mansri, A., Benmehdi, H., Meroufel, B., Desbrieres, J. and Dedriveres, R. (2011) Influence of pH on the uptake of toluene from water by the composite poly (4-vinylpyridinium)-maghnite. *African Journal of Pure and Applied Chemistry*, **5**, 486-493. [doi:10.5897/AJPAC11.066](https://doi.org/10.5897/AJPAC11.066)
- [11] Adebowale, K.O., Unuabonah, I.E. and Olu-Owolabi, B.I. (2006) The effect of some operating variables on the adsorption of lead and cadmium ions on kaolinite clay. *Journal of Hazardous Materials*, **134**, 130-139. [doi:10.1016/j.jhazmat.2005.10.056](https://doi.org/10.1016/j.jhazmat.2005.10.056)
- [12] Sarier, N. and Onder, E. (2010) Organic modification of montmorillonite with low molecular weight polyethylene glycols and its use in polyurethane nanocomposite foams. *Thermochimica Acta*, **510**, 113-121. [doi:10.1016/j.tca.2010.07.004](https://doi.org/10.1016/j.tca.2010.07.004)
- [13] Sarier, N., Onder, E. and Ersoy, S. (2010) The modification of Na-montmorillonite by salts of fatty acids: An easy intercalation process. *Colloids and Surfaces A: Physicochemical and Engineering Aspects*, **371**, 40-49. [doi:10.1016/j.colsurfa.2010.08.061](https://doi.org/10.1016/j.colsurfa.2010.08.061)
- [14] Desai, J.D., Pathan, H.M., Min, S.-K., Jung, K.-D. and Joo, O.S. (2005) FT-IR, XPS and PEC characterization of spray deposited hematite thin films. *Applied Surface Science*, **252**, 1870-1875. [doi:10.1016/j.apsusc.2005.03.135](https://doi.org/10.1016/j.apsusc.2005.03.135)
- [15] Leszczynska, A., Njuguna, J., Pielichowski, K. and Banerjee, J.R. (2007) Polymer/montmorillonite nanocomposites with improved thermal properties Part II. Thermal stability of montmorillonite nanocomposites based on different polymeric matrixes. *Thermochimica Acta*, **454**, 1-22
- [16] Abollino, O., Aceto, M., Malandrino, M., Sarzanini, C. and Mentasti, E. (2003) Adsorption of heavy metals on Na-montmorillonite. Effect of pH and organic substances. *Water Research*, **37**, 1619-1627. [doi:10.1016/S0043-1354\(02\)00524-9](https://doi.org/10.1016/S0043-1354(02)00524-9)
- [17] Gupta, S.S. and Bhattacharyya, K.G. (2008) Immobilization of Pb(II), Cd(II) and Ni(II) ions on kaolinite and montmorillonite surfaces from aqueous medium. *Journal of Environmental Management*, **87**, 46-58. [doi:10.1016/j.jenvman.2007.01.048](https://doi.org/10.1016/j.jenvman.2007.01.048)
- [18] Fan, Q.H., Shao, D.D., Hu, J., Wu, W.S. and Wang, X.K. (2008) Comparison of Ni<sup>2+</sup> sorption to bare and ACT-graft attapulgites: Effect of pH, temperature and foreign ions. *Surface Science*, **602**, 778-785. [doi:10.1016/j.susc.2007.12.007](https://doi.org/10.1016/j.susc.2007.12.007)
- [19] Wang, X.K., Chen, C.L., Hu, W.P., Ding, A.P., Xu, D. and Zhou, X. (2005) Sorption of 243Am(III) to multiwall carbon nanotubes. *Environmental Science & Technology*, **39**, 2856-2860. [doi:10.1021/es048287d](https://doi.org/10.1021/es048287d)
- [20] Tsai, S.C., Ouyang, S. and Hsu, C.N. (2001) Sorption and diffusion behavior of Cs and Sr on Jih-Hsing bentonite. *Applied Radiation and Isotopes*, **54**, 209-215. [doi:10.1016/S0969-8043\(00\)00292-X](https://doi.org/10.1016/S0969-8043(00)00292-X)
- [21] Bhattacharyya, K.G. and Gupta, S.S. (2008) Kaolinite and montmorillonite as adsorbents for Fe(III), Co(II) and Ni(II) in aqueous medium. *Applied Clay Science*, **41**, 1-9. [doi:10.1016/j.clay.2007.09.005](https://doi.org/10.1016/j.clay.2007.09.005)
- [22] Langmuir, I. (1918) The adsorption of gases on plane surfaces of glass, mica and platinum. *Journal of the American Chemical Society*, **40**, 1361-1403. [doi:10.1021/ja02242a004](https://doi.org/10.1021/ja02242a004)
- [23] Huang, Y.H., Hsueh, C.L., Cheng, H.P., Su, L.C. and Chen, C.Y. (2007) Thermodynamics and kinetics of adsorption of Cu(II) onto waste iron oxide. *Journal of Hazardous Materials*, **144**, 406-411.
- [24] Aydın, H., Bulut, Y. and Yerlikaya, C. (2008) Removal of copper (II) from aqueous solution by adsorption onto low-cost adsorbents. *Journal of Environmental Management*, **87**, 37-45. [doi:10.1016/j.jenvman.2007.01.005](https://doi.org/10.1016/j.jenvman.2007.01.005)
- [25] Weng, C.H., Tsai, C.Z., Chu, S.H. and Sharma, Y.C. (2007) Adsorption characteristics of copper(II) onto spent activated clay. *Separation and Purification Technology*, **54**, 187-197. [doi:10.1016/j.seppur.2006.09.009](https://doi.org/10.1016/j.seppur.2006.09.009)
- [26] Freundlich, H. (1906) Über die adsorption in lösungen. *Zeitschrift für Physikalische Chemie (Leipzig)*, **57**, 385-470.
- [27] Eren, E. (2008) Removal of copper ions by modified Unye clay, Turkey. *Journal of Hazardous Materials*, **159**, 235-244. [doi:10.1016/j.jhazmat.2008.02.035](https://doi.org/10.1016/j.jhazmat.2008.02.035)
- [28] Sari, A., Tuzen, M. and Soylak, M. (2007) Adsorption of Pb(II) and Cr(III) from aqueous solution on Celtek clay. *Journal of Hazardous Materials*, **144**, 41-46. [doi:10.1016/j.jhazmat.2006.09.080](https://doi.org/10.1016/j.jhazmat.2006.09.080)
- [29] Sari, A., Tuzen, M., Citak, D. and Soylak, M. (2007) Adsorption characteristics of Cu(II) and Pb(II) onto expanded perlite from aqueous solution. *Journal of Hazardous Materials*, **144**, 41-46. [doi:10.1016/j.jhazmat.2006.09.080](https://doi.org/10.1016/j.jhazmat.2006.09.080)

*dous Materials*, **148**, 387-394.

[doi:10.1016/j.jhazmat.2007.02.052](https://doi.org/10.1016/j.jhazmat.2007.02.052)

- [30] Xu, D., Tan, X.L., Chen, C.L. and Wang, X.K. (2008) Adsorption of Pb(II) from aqueous solution to MX-80 bentonite: Effect of pH, ionic strength, foreign ions and temperature. *Applied Clay Science*, **41**, 37-46.  
[doi:10.1016/j.clay.2007.09.004](https://doi.org/10.1016/j.clay.2007.09.004)
- [31] Günay, A., Arslankaya, E. and Tosun, I. (2007) Lead removal from aqueous solution by natural and pretreated clinoptilolite: Adsorption equilibrium and kinetics. *Journal of Hazardous Materials*, **146**, 362-371.  
[doi:10.1016/j.jhazmat.2006.12.034](https://doi.org/10.1016/j.jhazmat.2006.12.034)
- [32] Veli, S. and Alyüz, B. (2007) Adsorption of copper and zinc from aqueous solutions by using natural clay. *Journal of Hazardous Materials*, **149**, 226-233.  
[doi:10.1016/j.jhazmat.2007.04.109](https://doi.org/10.1016/j.jhazmat.2007.04.109)
- [33] Nunes, L.M. and Airoidi, C. (1999) Some features of crystalline  $\alpha$ -titanium hydrogenphosphate, modified sodium and *n*-butylammonium forms and thermodynamics of ionic exchange with  $K^+$  and  $Ca^{2+}$ . *Thermochimica Acta*, **328**, 297-305. [doi:10.1016/S0040-6031\(98\)00654-6](https://doi.org/10.1016/S0040-6031(98)00654-6)